X-ray and optical properties of broad absorption line quasars in the Canada-France-Hawaii Telescope Legacy Survey

C. S. Stalin, R. Srianand, P. Petitjean

X-ray and optical properties of broad absorption line quasars in the Canada–France–Hawaii Telescope Legacy Survey

C. S. Stalin,[1]★ R. Srianand[2] and P. Petitjean[3]

[1]*Indian Institute of Astrophysics, Block II, Koramangala, Bangalore 560034, India*
[2]*Inter-University Centre for Astronomy and Astrophysics, Post Bag 4, Ganeshkhind, 411007 Pune, India*
[3]*Institut d'Astrophysique de Paris, CNRS Université Pierre et Marie Curie, 98bis bd Arago, Paris 75014, France*

ABSTRACT

We study the X-ray and optical properties of 16 broad absorption line (BAL) quasars detected in a $\approx 3\,\deg^2$ region common to the wide synoptic (W-1) component of the Canada–France–Hawaii Telescope Legacy Survey (CFHTLS) and the *XMM* Large Scale Structure Survey (XMM-LSS). The BAL fraction is found to be 10 per cent in the full sample, 7 per cent for the optical colour-selected quasi-stellar objects (QSOs) and as high as 33 per cent if we consider QSOs selected from their infrared colours. The X-ray-detected non-BAL and BAL quasars have a mean observed X-ray-to-optical spectral slope ($\alpha_{\rm ox}$) of -1.47 ± 0.13 and -1.66 ± 0.17, respectively. We also find that the BAL QSOs have $\alpha_{\rm ox}$ systematically smaller than what is expected from the relationship between optical luminosity and $\alpha_{\rm ox}$ as derived from our sample. Based on this, we show, as already reported in the literature for quasars with high optical luminosities, that our new sample of BAL QSOs has X-ray luminosity a factor of 3 smaller than what has been found for non-BAL QSOs with similar optical luminosities. Comparison of hardness ratios of the BAL and non-BAL QSOs suggests a possible soft X-ray weakness of BAL QSOs. Combining our sample, of relatively fainter QSOs, with others from the literature we show that larger balnicity index (BI) and maximum velocity ($V_{\rm max}$) of the C IV absorption are correlated with steeper X-ray-to-optical spectral index. We argue that this is most likely a consequence of the existence of a lower envelope in the distribution of BI (or $V_{\rm max}$) values versus optical luminosity. Our results thus show that the previously known X-ray weakness of BAL QSOs extends to lower optical luminosities as well.

Key words: surveys – galaxies: active – quasars: general – X-rays: general.

1 INTRODUCTION

Broad absorption line (BAL) quasars are active galactic nuclei (AGN) characterized by the presence of strong absorption troughs in their ultraviolet (UV) spectra. They constitute an observed fraction of about 10–15 per cent of optically selected quasars (Hewett & Foltz 2003; Reichard et al. 2003). Recently, it has been shown that the actual BAL fraction could be higher as optical colour selection of quasi-stellar objects (QSOs) may be biased against the BAL QSOs (see for example Dai, Shankar & Sivakoff 2008; Shankar, Dai & Sivakoff 2008; Urrutia et al. 2009; Allen et al. 2010) The BALs are attributed to material flowing outwards from the nucleus with velocities of 5000–50 000 km s^{-1} (Green et al. 2001). These quasars are classified into three subclasses based on the material producing the BAL troughs. High-ionization BAL quasars (HiBALs) have broad absorption from C IV, Si IV, N V and O VI. About 10 per cent

of BAL quasars also show, apart from their HiBAL features, broad absorption lines of lower ionization species such as Mg II or Al III and are called low-ionization BAL quasars (LoBALs). Finally, LoBALs with absorptions from excited states of Fe II or Fe III are called FeLoBALs (Wampler, Chugai & Petitjean 1995). BAL quasars in general have higher optical-UV polarization than non-BAL quasars, and the LoBALs tend to have particularly high polarization than HiBALs (Hutsemekers, Lamy & Remy 1998; Schmidt & Hines 1999; DiPompeo et al. 2010). LoBALs have a more reddened optical continuum compared to non-BAL and HiBAL QSOs (Sprayberry & Foltz 1992; Becker et al. 2000), thereby suggesting the presence of larger amounts of dust in them. In X-rays too, LoBALs have higher absorbing column densities than HiBALs (Green et al. 2001; Gallagher et al. 2002).

The dichotomy between BAL and non-BAL quasars is often thought to be a consequence of orientation. The similarity between the optical/UV emission lines and continuum properties of BAL and non-BAL quasars (Weymann et al. 1991; Reichard et al. 2003) supports a scenario where the observed fraction of BAL quasars

★E-mail: stalin@iiap.res.in

corresponds to the covering fraction of a wind that could be present in all AGN. Earlier spectropolarimetric observations too support this orientation scheme (Goodrich & Miller 1995; Hines & Wills 1995). However, recent spectropolarimetric observations of radio-loud BALs do not favour the orientation-dependent scheme for the BAL phenomenon (DiPompeo et al. 2010). On the other hand, Allen et al. (2010) found a strong redshift dependence of the C IV BAL quasar fraction. They conclude that the BAL phenomenon cannot be due to an orientation effect only. Alternative to the orientation scheme, it is argued that the observed BAL quasar fraction could correspond to the intrinsic fraction of quasars hosting massive nuclear winds, thereby tracing an evolutionary phase of the AGN lasting $\approx$10–15 per cent of their lives (Hazard et al. 1984; Becker et al. 2000; Giustini, Cappi & Vignali 2008). In this scenario, the large amounts of gas and dust surrounding the central source should lead to enhanced far-infrared (IR) and submillimetre emission in BAL quasars with respect to non-BAL quasars (Giustini et al. 2008). However, submillimetre studies found no (Willott, Rawlings & Grimes 2003) or little (Priddey et al. 2007) differences between the two populations. Also, the mid-IR properties of BAL and non-BAL quasars of comparable luminosities are indistinguishable (Gallagher et al. 2007). BAL quasars are predominantly radio quiet, while few radio-loud BAL quasars are also known (Becker et al. 2000; Brotherton et al. 2005).

Although radiative acceleration could be the main driving mechanism in BAL quasars (Arav, Li & Begelman 1994; Srianand et al. 2002), we still do not have a clear picture of the physics of outflows/winds in BALs. X-ray observations can help constrain the physical mechanisms at play in BAL quasar outflows and the different scenarios proposed (Giustini et al. 2008). Since the *ROSAT* survey, BAL quasars which are radio quiet have been known to have faint soft X-ray-to-optical luminosity ratio (Green et al. 1995; Green & Mathur 1996). Their X-ray luminosity is typically 10–30 times lower than expected from their UV luminosity, qualifying them as soft X-ray weak objects (Laor et al. 1997). This implies that the soft X-ray continuum of BAL quasars is either (i) strongly absorbed by highly ionized material or (ii) intrinsically underluminous. Given the extreme absorption evident in the UV, this soft X-ray faintness was assumed to result from intrinsic absorption in BAL material of high column density, typically $N_H > 10^{22}$ cm^{-2} (Green et al. 1995, 2001; Brotherton et al. 2005; Gallagher et al. 2006, hereafter G06; Fan et al. 2009; Gibson et al. 2009). However, it has also been argued that intrinsic X-ray faintness cannot be ruled out as the cause for their observed X-ray weakness (Mathur et al. 2000; Sabra & Hamann 2001; Gupta et al. 2003; Ghosh & Punsly 2008; Giustini et al. 2008; Wang et al. 2008). Radio-loud BAL quasars are also found to be X-ray weak when compared with radio-loud non-BAL quasars of similar UV/optical luminosities (Miller et al. 2009).

X-ray spectral analysis of BAL quasars considering neutral and ionized absorbers are found to yield low neutral hydrogen ($N_H < 10^{21}$ cm^{-2}) and high ionized hydrogen ($N_H^i > 10^{21}$ cm^{-2}) column density, respectively (Giustini et al. 2008; Streblyanska et al. 2010). It thus seems that the inferred N_H values depend on (i) the ionization state of the gas in our line of sight to the BAL quasar and (ii) the absorber either fully or partially covering the X-ray source. Here, we investigate the issue of the X-ray weakness of BAL quasars using a new sample of quasars selected in the Canada–France–Hawaii Telescope Legacy Survey (CFHTLS[1]) and overlapping the *XMM* Large Scale Structure Survey (XMM-LSS) and the *Spitzer*

Wide-area InfraRed Extragalactic (SWIRE) survey with the aims of (i) identifying a homogeneous sample of BAL quasars from a parent quasar sample and (ii) studying the X-ray nature of those identified BAL quasars. The sample has been selected without a prior knowledge of the BAL nature of the objects. This paper is organized as follows. The data set used and the observations are described in Section 2. Identification of BAL quasars is given in Section 3. Results of the analysis are presented in Section 4, and the conclusions are drawn in Section 5. Throughout this paper, we adopt a cosmology with $H_0 = 70$ km s^{-1} Mpc^{-1}, $\Omega_m = 0.27$ and $\Omega_\Lambda = 0.73$.

2 DATA SET

The optical data set used in this work is from the wide synoptic (W-1) component of CFHTLS. CFHTLS images are available in five optical bands (u^*, g', r', i' and z') down to $i'_{AB} = 24$ mag. The field has been observed in the course of the XMM-LSS. Centred at ($\alpha_{2000} = 37.5$, $\delta_{2000} = -5°$), the XMM-LSS (Pierre et al. 2004) is a medium-depth large-area X-ray survey designed to map the large-scale structures in the nearby Universe. The catalogue for the first 5.5 deg^2 (pertaining to 45 *XMM* pointings) observed in the 0.5–2 and 2–10 keV bands, listing sources above a detection likelihood of 15 in either bands, was released by Pierre et al. (2007). Also, overlapping the XMM-LSS and CFHTLS fields is the SWIRE survey (Lonsdale et al. 2003).

We are in the process of carrying out optical spectroscopic identification of quasar candidates selected in about 10 deg^2 in the W-1 region. Some regions of W-1 also have coverage from the XMM-LSS and the SWIRE survey. Therefore, several selection criteria were adopted to select quasar candidates, namely (i) optical colour–colour criteria similar to that used in Sloan Digital Sky Survey (SDSS; Richards et al. 2002), (ii) IR colour–colour criteria following Stern et al. (2005) and (iii) optical spectral energy distribution (SED) matching using the photometric redshift code HYPERZ (Bolzonella, Miralles & Pellò 2000). Our final list of quasar candidates in W-1 thus consists of (1) candidates selected both by optical colour and template-matching criteria, (2) candidates selected by optical colour but missed by template-matching method, (3) candidates selected by optical template-matching method but missed by optical colour selection (4) candidates selected by IR colour selection but missed in optical selection and (5) all *XMM* sources having optical counterparts but not selected through (1), (2), (3) and (4). Our candidate selection was limited to sources brighter than $g' < 22$ mag. A complete description of our procedure of quasar candidate selection as well as the results of the quasar-selection efficiency will be discussed in a forthcoming paper (Stalin et al., in preparation) when our complete quasar survey will be reported. Our main aim here is to understand the X-ray and optical properties of BAL quasars. Thus, for this work, we have considered only $\approx$3 deg^2 region in W-1, which has both optical and X-ray-imaging observations. This region is shown as a large circle in Fig. 1. Also, marked on this figure are the regions covered by the XMM-LSS and the SWIRE survey.

Optical spectroscopic observations of the quasar candidates selected in the $\approx$3 deg^2 circular region shown in Fig. 1 were carried out with the AAOmega system (Sharp et al. 2006) on the 3.9-m AAT, during two observing runs in September 2006 and 2007. The field of the camera has a diameter of 2° and was centred at $\alpha_{2000} = 36.15$ and $\delta_{2000} = -4.50$ (see Fig. 1). The 580V and 385R gratings were used, respectively, in the blue and red arms of the spectrograph, thereby simultaneously covering the wavelength range 3700–8800 Å and
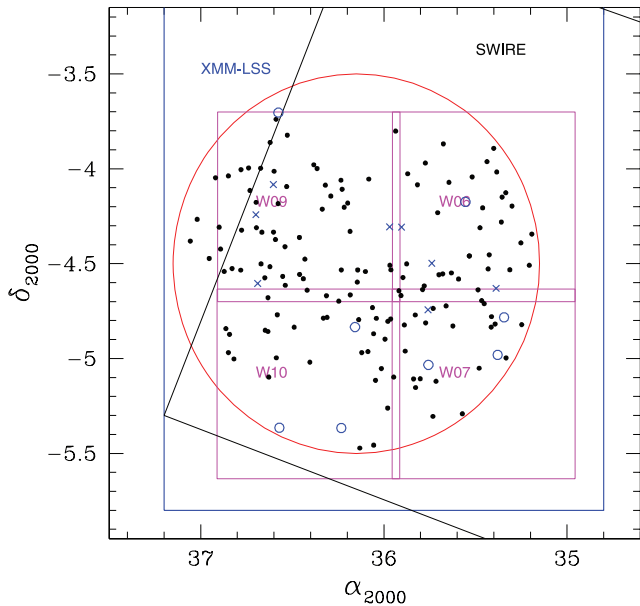
[1] http://www.cfht.hawaai.edu/Science/CFHTLS/

Figure 1. Layout of the field used to select quasars in this study. The XMM-LSS and the SWIRE survey regions are delineated. W06, W07, W09 and W10 are the four pointings of CFHTLS and the large circle is the $\sim$3 deg^2 region searched for quasars in this work. The quasars are marked as filled circles, the BAL quasars detected in X-ray are shown as crosses and the BAL quasars undetected in X-rays are shown as open circles.

delivering a spectral resolution of $R \sim 1300$. The total integration time ranged from 30 min to 3 h depending on the brightness of the candidates.

Spectroscopic data reduction was performed using the AAOmega's data reduction pipeline software DRCONTROL. The two-dimensional images were flat fielded, and the spectra were extracted (using a Gaussian profile extraction), wavelength calibrated and combined within DRCONTROL. Redshifts were derived using the AUTOZ code (kindly provided to us by Scott Croom). Individual QSO spectra were manually checked to confirm the correctness of the redshift. Further details of the observations and reductions can be found in Stalin et al. (2010).

A total of 159, $z_{em} > 1.5$, new quasars were identified from the AAT observations in $\approx$3 deg^2. They are shown as filled circles in Fig. 1. This is the sample we use here to investigate the X-ray properties of BAL and non-BAL quasars. Note that the above redshift cut-off is necessary in order to observe the C IVλ1549 BAL feature in the spectral range 3800–8800 Å. Out of these 159 quasars, 120 were primarily selected based on optical colour selection without any prior knowledge of X-ray emission, 12 sources were selected based on their IR colour (also without any knowledge of X-rays) from the SWIRE survey but were missed by our optical selection and 27 sources were selected from the *XMM* source list through the presence of X-ray emission. We find 72 per cent (i.e. 86 quasars out of 120) of the optically selected quasars are also detected in *XMM*. However, only 33 per cent (i.e. four quasars our of 12) of the IR-only-selected candidates are detected by *XMM*. All of the 120 optically colour-selected quasars were detected by the SWIRE survey in one of the five IR bands. However, only 78 of these 120 sources have IR flux values in all the four IR bands so that IR selection criteria can be applied to them. Of these 78, 77 are also IR colour–colour selected. The average $u' - g'$ and $g' - r'$ colours of the 12 IR-only-selected quasars are redder than that of the 120 optically colour-selected quasars.

3 IDENTIFYING BALs

From our sample of 159 quasars, we initially identified quasars with broad C IV absorption close to the emission redshift by eye. We then calculated the balnicity index (BI) for these quasars as defined by Weymann et al. (1991),

$$\mathrm{BI} = -\int_{25000}^{3000} \left[1 - \frac{f(v)}{0.9} \right] C \mathrm{d}v. \qquad (1)$$

Here, $f(v)$ is the continuum-normalized flux at a velocity v (in km s^{-1}) defined with respect to the quasar rest frame. The dimensionless value C is initially set to zero. It is set to 1.0 whenever the quantity in brackets has been continuously positive over an interval of 2000 km s^{-1}. Traditionally, BAL quasars are defined as quasars with BI > 0. We fitted a smooth continuum to these quasar spectra using the method similar to the one described in Trump et al. (2006). The normalized spectrum is used to measure BI. We also simultaneously estimated V_{max}, the maximum outflow velocity at which $f(v)$ is 0.9. The properties of the 16 new BAL (all HiBALs) quasars with BI >100 km s^{-1} are summarized in Table 1. They are shown as crosses (BALs detected in X-rays in the XMM-LSS) and open circles (BALs undetected in X-rays in the XMM-LSS) in Fig. 1. Of these 16 BAL quasars, we have Mg II coverage for six BAL quasars. None of these six BALs is found to be LoBALs. This is not surprising, as we would expect to see 1.6 LoBALs if all the 16 BALs had Mg II coverage in their spectra, as only 10 per cent of optically selected BALs are known to be LoBALs.

We find a BAL quasar fraction $f_{BAL} = N(\mathrm{BAL})/N(\mathrm{Total}) \approx 10 \pm 3$ per cent in our sample. If we restrict ourselves to the optical colour-selected quasars, we find 8 ± 3 per cent of them are BAL quasars. We also find 7 ± 5 per cent of the *XMM*-selected quasars to be BAL quasars. This is consistent with the rate found for the optical colour-selected candidates. There are 12 quasars which are selected via IR colour selection but are not part of our optical colour selection. Out of these 12 quasars, four are found to be BAL quasars. We thus find a BAL detection rate of 33 ± 19 per cent among the IR-only-selected quasars.

In our sample of optically selected quasars, the observed BAL quasar fraction is very similar to the fraction 10–15 per cent reported in the literature from optically selected quasar samples (see Weymann et al. 1991; Tolea, Krolik & Tsvetanov 2002; Hewett & Foltz 2003; Reichard et al. 2003; Trump et al. 2006; Knigge et al. 2008; Gibson et al. 2009). However, the BAL quasar fraction found in optically selected sample could not represent the true BAL fraction. This is because optical surveys will miss BAL quasars as their optical broad-band colours are affected by reddening in their UV spectra and large absorption in their BAL troughs. This is clearly evident in the higher BAL quasar fraction of 23 ± 3 per cent reported by Dai et al. (2008) in the Two Micron All Sky Survey (2MASS) selected quasars. When Hewett & Foltz (2003) considered the effect of reddening in their BAL quasars sample, they found a BAL quasar fraction of 22 per cent similar to that of Dai et al. (2008). High BAL quasar fraction is also claimed in the samples selected based on radio emission (see Shankar et al. 2008; Urrutia et al. 2009). Interestingly, this is also consistent with the higher BAL quasar fraction we find among the objects selected from IR colours only. Note that Dai et al. (2008) argued that the selection based on optical colours has significant selection biases against BAL quasars, and the BAL quasar fraction in NIR colour-selected sample more accurately reflects the true fraction of BAL quasars. Indeed, Allen et al. (2010) have shown that, when the incompleteness related to the BAL identification in the SDSS spectrum and the colour

Table 1. Properties of BAL quasars in CFHTLS.

RA (h m s)	Dec. (° ′ ″)	g' (mag)	α_{ox}	$\Delta\alpha_{ox}$	$L_{0.5-2\,keV}$ (erg s^{-1})	$L_{2\,keV}$ (erg s^{-1} keV^{-1})	$L_{2500\,\text{Å}}$ (erg s^{-1} Å^{-1})	z	V_{max} (km s^{-1})	BI
02:23:02.278	−04:44:37.057	19.89	−1.94	−0.466	43.50	26.36	30.82	2.03	10335.0	3200.0
02:23:52.537	−04:18:21.620	20.54	−1.83	−0.354	43.51	26.37	30.54	2.05	5701.0	2126.0
02:26:24.710	−04:04:59.075	19.84	−1.63	−0.119	44.48	26.77	31.00	2.52	19409.0	500.0
02:26:47.693	−04:14:30.763	20.78	−1.63	−0.152	44.06	26.34	30.59	2.33	8233.0	6065.0
02:26:45.443	−04:36:15.475	19.92	−1.72	−0.174	44.84	27.17	31.66	3.28	22440.0	6567.0
02:22:57.309	−04:29:52.856	21.68	−1.56	−0.119	43.66	25.90	29.96	1.84	4308.0	580.0
02:21:33.091	−04:37:48.852	21.45	−1.54	−0.047	44.45	26.76	30.77	2.99	3942.0	109.0
02:23:36.896	−04:18:27.431	21.24	−1.41	0.056	44.46	26.77	30.46	2.96	5569.0	479.0
02:24:55.759	−05:21:59.772	19.93	<−1.94	<−0.420	<43.86	<26.77	31.23	2.85	23766.0	3376.0
02:26:16.910	−05:21:52.820	20.39	<−1.79	<−0.309	<43.70	<26.59	30.65	2.45	6139.0	1742.0
02:22:13.311	−04:10:30.093	20.24	<−1.84	<−0.372	<43.43	<26.28	30.48	1.90	20640.0	2546.0
02:24:37.908	−04:50:02.572	20.42	<−1.85	<−0.375	<43.41	<26.26	30.46	1.87	4380.5	422.0
02:21:22.497	−04:46:58.606	20.43	<−1.84	<−0.345	<43.78	<26.67	30.88	2.63	10964.0	3620.0
02:26:18.182	−03:42:15.797	20.68	<−1.77	<−0.299	<43.61	<26.48	30.50	2.25	10053.0	4640.0
02:21:30.978	−04:58:52.086	21.95	<−1.56	<−0.105	<43.85	<26.75	30.22	2.81	4781.0	2996.0
02:23:01.742	−05:01:59.748	20.96	<−1.78	<−0.313	<43.46	<26.31	30.34	1.95	14430.0	6061.0

selection method used to identify QSOs were taken into account, the actual BAL fraction can be as high as 41 ± 5 per cent instead of 8.0 ± 0.1 per cent found from the SDSS sample.

Of the 16 BAL quasars in our sample, eight are detected in the XMM-LSS (50 ± 22 per cent). Even if we restrict the sample to the colour-selected objects, we find equal numbers of BAL quasars with and without detectable X-ray emission (i.e. 50 per cent). The spectra of the eight BAL quasars that are detected by *XMM* in the XMM-LSS are shown in Fig. 2. Fig. 3 shows the spectra of the remaining eight BAL quasars that are not detected in the XMM-LSS. Our X-ray-detection rate is slightly lower than the 77 ± 20 per cent reported by G06, 74 ± 13 per cent reported by Gibson et al. (2009) and 63 ± 16 per cent reported by Fan et al. (2009). However, within uncertainties our value matches well with that from previous studies. There are two main differences between our study and the above listed studies. First, our sample is optically selected and then correlated with the XMM-LSS, thereby making BAL and non-BAL quasars have similar X-ray flux limits. Secondly, the quasars in our study are typically fainter than those used in the other three studies (see Fig. 5). It is also interesting to note that on an average, objects in the sample of G06 are optically more luminous than those of Fan et al. (2009). Similarly, objects in our sample are systematically fainter than the sample considered by Fan et al. (2009).

There are seven radio-loud quasars in our sample (see table 5 of Stalin et al. 2010). None of them is a BAL quasar. Using the BAL fraction found by Shankar et al. (2008) for radio-selected quasars, we should expect 1.5 radio-loud BAL quasars.

4 PROPERTIES OF BAL QUASARS IN OUR SAMPLE

4.1 Optical-to-X-ray spectral index (α_{ox})

The broad-band spectral index α_{ox} is generally used to quantify the relative UV-to-X-ray power of the quasar. We estimated α_{ox} for each of the spectroscopically identified AGN in our sample. For this, we have converted the observed i'-band magnitudes to fluxes following the definition of the AB system (Oke & Gunn 1983):

$$S_{i'} = 10^{-0.4(m_{i'}+48.60)}, \qquad (2)$$

where $S_{i'}$ and $m_{i'}$ are, respectively, the flux and magnitude in the i' band. The luminosity at the frequency corresponding to 2500 Å in the rest frame is calculated following Stern et al. (2000),

$$L_{\nu_1} = \frac{4\pi D_1^2}{(1+z)^{1+\alpha_o}} \left(\frac{\nu_1}{\nu_2}\right)^{\alpha_o} S_{\nu_2}, \qquad (3)$$

where ν_2 is the observed frequency corresponding to the i' band, S_{ν_2} is the observed flux in i' band, ν_1 is the rest-frame frequency corresponding to 2500 Å and D_1 is the luminosity distance. An optical spectral index $\alpha_o = -0.5$ (Anderson et al. 2007) is assumed ($S_\nu \propto \nu^\alpha$). The luminosity at 2 keV in the rest frame is obtained using a similar equation as equation (3), assuming a X-ray spectral index of $\alpha_x = -1.5$ (Anderson et al. 2007).

Thus, the broad-band spectral index α_{ox} is obtained as

$$\alpha_{ox} = \frac{\log(L_{2\,keV}/L_{2500\,\text{Å}})}{\log(\nu_X/\nu_{opt})}. \qquad (4)$$

Here $L_{2\,keV}$ and $L_{2500\,\text{Å}}$ are the rest-frame monochromatic luminosities (in erg s^{-1} Hz^{-1}) at $\nu_X = 2$ keV and ν_{opt}, respectively, corresponding to 2500 Å.

Fig. 4 shows the distribution of observed α_{ox} (not corrected for intrinsic and Galactic absorption) for the sample of the *XMM*-detected non-BAL and BAL quasars. The BAL quasars have systematically lower values of α_{ox} compared to the non-BAL quasars. We find a mean $\alpha_{ox} = -1.47 \pm 0.13$ and -1.66 ± 0.17 for the *XMM*-detected non-BAL and BAL quasars, respectively. In our sample, the upper limits of α_{ox} derived for the *XMM*-undetected BALs are towards the lower end of the distribution of α_{ox} found for the *XMM*-detected non-BAL quasars as can be seen in Fig. 4.

We now compare our results with other BAL quasar studies. In Fig. 5, we show the distribution of $L_{2500\,\text{Å}}$ luminosity and α_{ox} for our sample of BAL quasars as well as other quasar samples published in the literature. Objects in our sample are systematically fainter than those in the published samples, namely G06, Fan et al. (2009), Giustini et al. (2008) and Gibson et al. (2009). The α_{ox} distribution of our sample has some overlap with Fan et al. (2009), Giustini et al. (2008) and Gibson et al. (2009) samples but is offset from the distribution of G06. G06 found a median α_{ox} of -2.20, which is much smaller than that found by Fan et al. (2009), Giustini et al. (2008) and Gibson et al. (2009). The objects in the G06 sample are luminous, and the low value of α_{ox} found might be due to
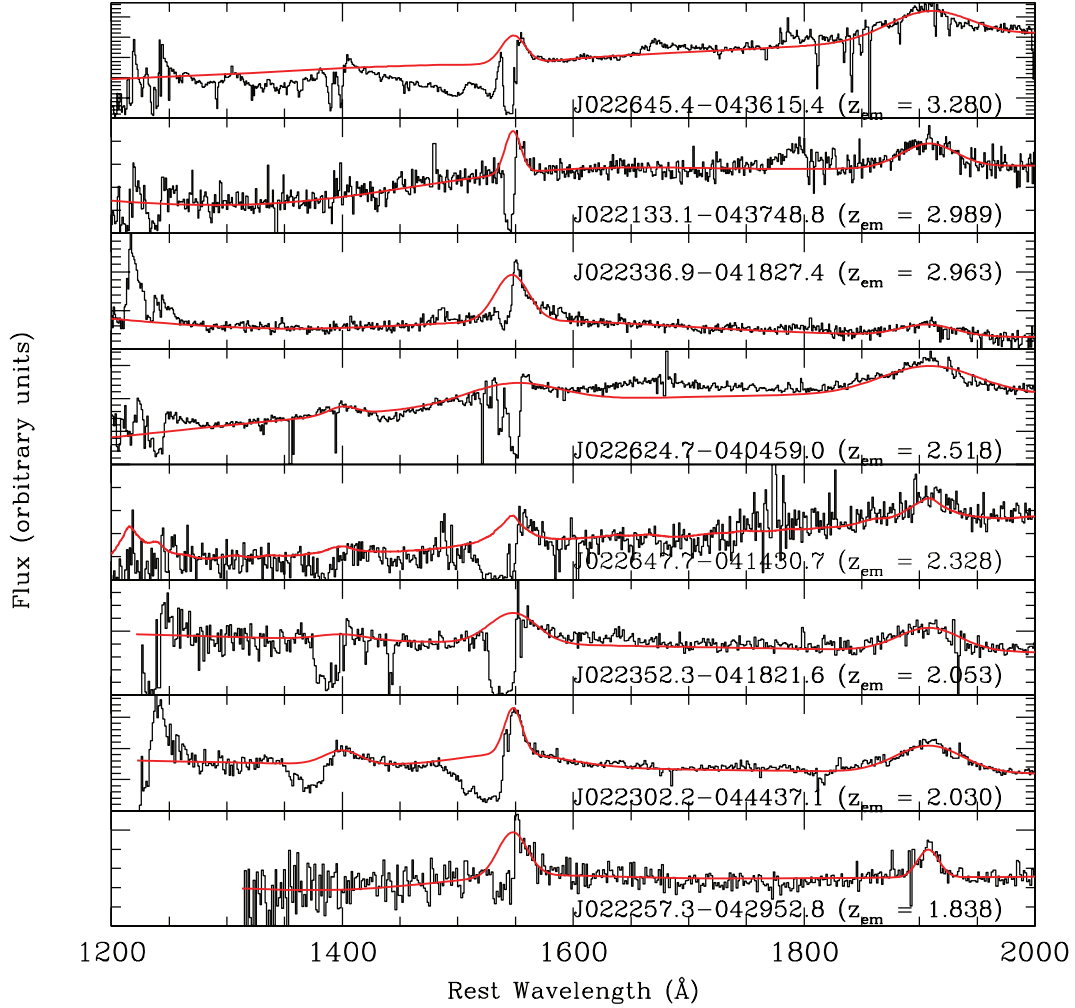
Figure 2. The rest-frame spectra of BAL quasars detected by *XMM* in our sample. The best-fitting continuum is over-plotted.

the dependence of $\alpha_{\rm ox}$ on luminosity reported by various authors (Steffen et al. 2006; Just et al. 2007; Green et al. 2009). Recently, for CFHTLS quasars, Stalin et al. (2010) found a dependence of $\alpha_{\rm ox}$ on $L_{2500\,\text{Å}}$ and is given by

$$\alpha_{\rm ox} = (-0.065 \pm 0.019)\log(L_{2500}) + (0.509 \pm 0.560). \tag{5}$$

This relation is in agreement to that found by Green et al. (2009), however, flatter than the value found by Steffen et al. (2006) and Just et al. (2007). To overcome this dependence of $\alpha_{\rm ox}$ on $L_{2500\,\text{Å}}$ luminosity, we study the distribution of $\Delta\alpha_{\rm ox}$ values for our sample. For calculating $\Delta\alpha_{\rm ox}$ values, we opted to use the relation between $\alpha_{\rm ox}$ and $L_{2500\,\text{Å}}$ obtained by Stalin et al. (2010) for the CFHTLS quasars. $\Delta\alpha_{\rm ox}$ is defined as the difference between the observed $\alpha_{\rm ox}$ and $\alpha_{\rm ox}(L_{2500\,\text{Å}})$ calculated using equation (5) given the optical luminosity of the object. This gives an estimate of how the X-ray luminosity of a BAL quasar differs from that of a typical non-BAL quasar of the same $L_{2500\,\text{Å}}$. For BAL quasars culled from literature, $\Delta\alpha_{\rm ox}$ was recalculated using equation (5). The distributions of $\Delta\alpha_{\rm ox}$ for our sample of BAL and non-BAL quasars are shown in Fig. 6. In the case of the *XMM*-detected non-BAL quasars, $\Delta\alpha_{\rm ox}$ is found to be distributed symmetrically around zero. On the contrary, the distribution of $\Delta\alpha_{\rm ox}$ for the *XMM*-detected BAL quasars is offset from zero. The average $\Delta\alpha_{\rm ox}$ for the *XMM*-detected non-BAL and BAL quasars are 0.005 ± 0.119 and -0.169 ± 0.161, respectively.

Using equation (5), we can say that $\Delta\alpha_{\rm ox}$ of -0.169 corresponds to an X-ray luminosity weaker by a factor of $\sim$3 with respect to typical non-BAL quasars of the same $L_{2500\,\text{Å}}$. Thus, in our sample, BAL quasars appear to be X-ray weak compared to their non-BAL counterparts. This is similar to what some previous studies have reported (G06; Fan et al. 2009; Gibson et al. 2009).

4.2 Correlation between X-ray and UV properties

Models of BAL outflows based on radiation-driven flows predict a correlation between the outflow velocity ($V_{\rm max}$) and the quasar luminosity (Arav et al. 1994). The transfer of photon momentum depends on the column density and the ionization state of the absorbing gas. The ionization state of the BAL outflow very much depends on the optical-to-soft-X-ray SED of the ionizing continuum (Srianand & Petitjean 2000; Gupta et al. 2003). In order for an efficient transfer of radiative momentum to the absorbing gas, it is important that the gas is not overionized despite being very close to the central engine (see Proga, Stone & Kallman 2000). This can be achieved if there is a highly ionized (not seen in UV absorption) gas component at the base of the flow that shields X-rays from the UV-absorbing gas (Murray & Chiang 1995). In such a scenario, one would expect the properties of the UV-absorbing gas to be related to the properties of the X-ray-absorbing gas at the base of the same
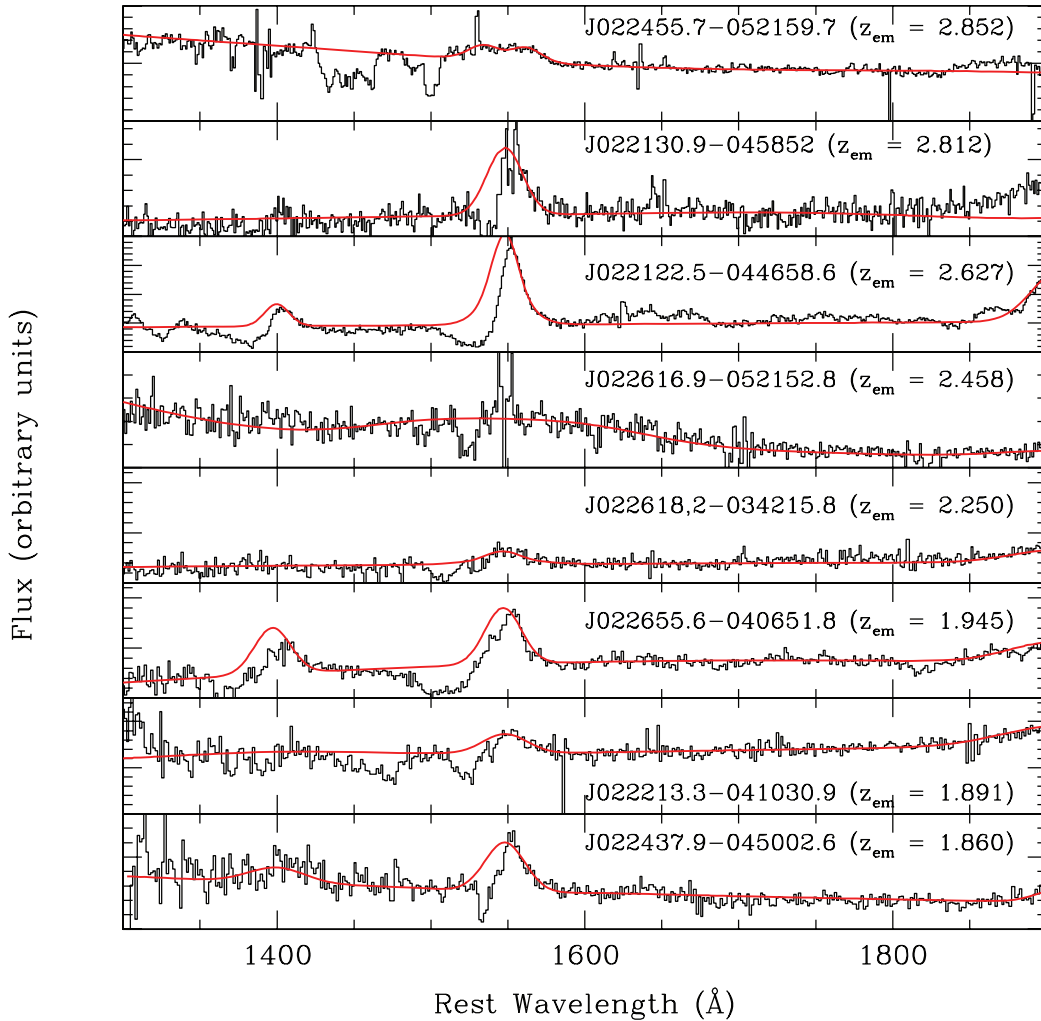
Figure 3. The rest-frame spectra of BAL quasars in our sample without X-ray detection. The best-fitting continuum is over-plotted.

flow. We therefore investigate correlations between the kinematical properties of UV absorptions (V_{max} and BI) with $\Delta\alpha_{ox}$, an indicator of X-ray absorption, and $L_{2500\,Å}$. For these statistical study, we add to the new BAL quasars reported in this work HiBALs from the literature. We have included 29 BAL QSOs from G06, 38 BAL QSOs from Giustini et al. (2008), 42 BAL QSOs from Gibson et al. (2009) and 35 BAL QSOs from Fan et al. (2009). Thus our extended sample consists of 160 high ionization BAL QSOs. Even though our new BAL quasars constitute only 10 per cent of the extended sample, it is significant to the statistical analysis as they are systematically fainter in optical luminosity than the ones from the literature.

In Fig. 7, we plot the BI measured from the C IV absorption against $\Delta\alpha_{ox}$ for the enlarged sample of BAL quasars including our own 16 BAL quasars. In our sample, two out of three of the BALs with BI > 5000 km s^{-1} show $-0.2 \leq \Delta\alpha_{ox} \leq -0.1$. However, among objects with BI $\geq$ 2000 km s^{-1}, only four out of 10 BAL QSOs show X-ray detection, whereas four out of five objects with $100 \leq$ BI ≤ 1000 km s^{-1} are detected in X-rays. Thus there appears to be a tendency of QSOs with large BI values to be weaker in X-rays. Now, we explore this correlation in the extended sample discussed above. As BI values are not available for the objects in Giustini et al. (2008), the corresponding objects are not considered in the analysis. In Fig. 7, we plot $\Delta\alpha_{ox}$ against BI for all the remaining 122 objects in the combined sample. The Kendall τ-test as implemented in the

ASURV (Astronomy Survival Analysis) package (Lavalley, Isobe & Feigelson 1992), which treats both upper and lower limits, gives a probability of <0.01 per cent that the two variables are uncorrelated (see Table 2). This is consistent with a 99.95 per cent correlation found by Fan et al. (2009) between BI and $\Delta\alpha_{ox}$ (see also Gibson et al. 2009). From Fig. 7, it can be readily seen that most of the G06 sources have high BI occupying the top left-hand corner of the diagram. To check if the derived correlation is dominated by the G06 sources, we applied the test without these sources. This time too, a correlation is noted, with the Kendall τ-test giving a probability of 0.01 per cent that BI and $\Delta\alpha_{ox}$ are uncorrelated (Table 2). This is mainly due to the fact that we have only upper limits on $\Delta\alpha_{ox}$ in most QSOs with BI > 1000 km s^{-1}.

Next we look for the correlations between V_{max} and $\Delta\alpha_{ox}$. There is no apparent trend between the two if we consider only our sample. The objects with upper limits on $\Delta\alpha_{ox}$ are spread over the whole V_{max} range. In Fig. 8, we plot V_{max} measured from the C IV absorption versus $\Delta\alpha_{ox}$ in the extended BAL quasar sample. The Kendall τ-test gives a probability of <0.01 per cent that the two variables are not correlated (Table 2). In the past, different samples have given different results for this correlation. G06 and Gibson et al. (2009) have found significant correlation between V_{max} and $\Delta\alpha_{ox}$, but this was not confirmed by Fan et al. (2009) and Giustini et al. (2008). In the extended sample, even when we remove the points from G06,
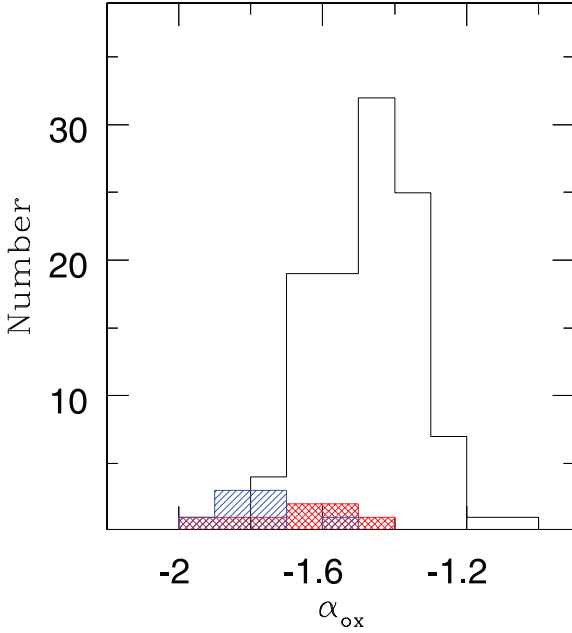
Figure 4. Distributions of α_{ox} in our sample. The solid histogram is for the *XMM*-detected non-BAL quasars. The hashed histogram is for the *XMM*-detected BAL quasars and the shaded histogram shows the upper limits of α_{ox} for the X-ray-undetected BAL quasars.
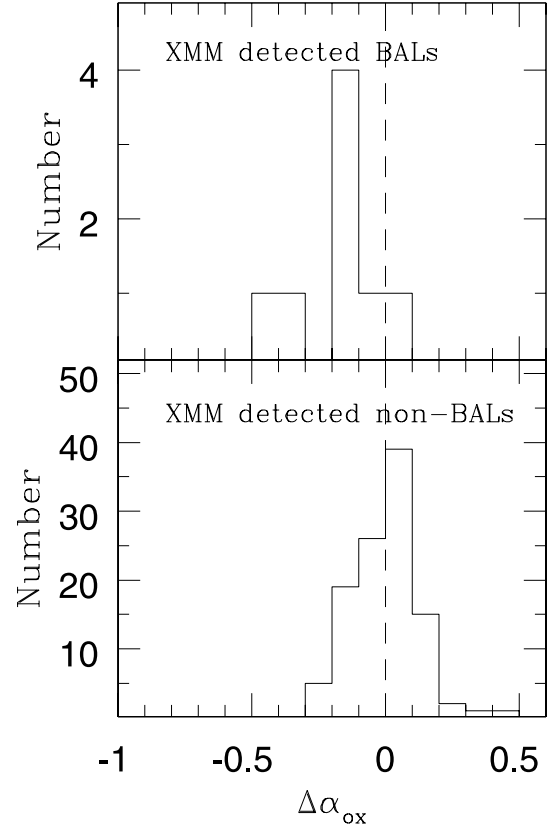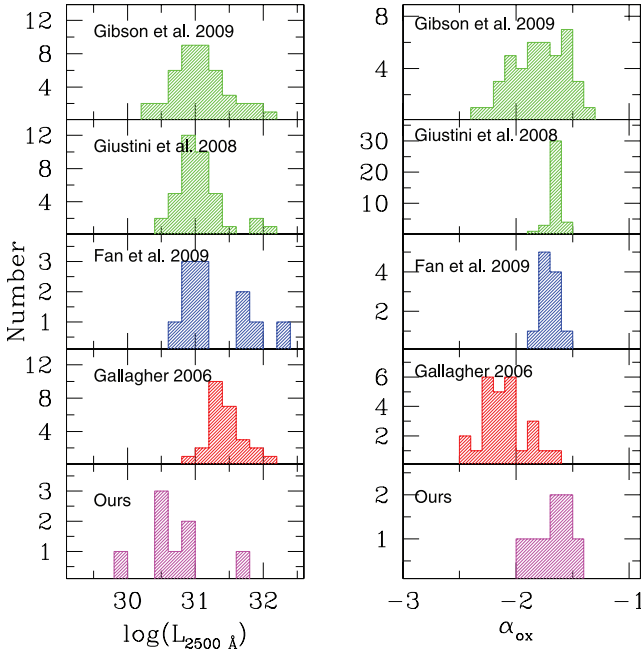

Figure 5. Distribution of the monochromatic luminosity at 2500 Å (left-hand panel) and α_{ox} (right-hand panel) in several BAL quasar samples. The references from where the samples are taken are given in each panel.

Figure 6. Distributions of $\Delta\alpha_{ox}$ in our sample. The top panel is for the *XMM*-detected BAL quasars and the bottom panel is for the *XMM*-detected non-BAL quasars.

we do find a very small Kendall probability ($P < 0.01$ per cent) that the two parameters are not correlated (see Table 2). If we remove points from Giustini et al. (2008), because they are not selected homogeneously, the Kendall τ-test gives a probability of <0.01 per cent that V_{max} and $\Delta\alpha_{ox}$ are uncorrelated.

It is a fact that the points in Figs 7 and 8 appear to be scattered even though the Kendall τ-test hints at the existence of a possible correlation between $\Delta\alpha_{ox}$ and kinematical parameters derived from

the UV absorptions. This is mainly due to the paucity of points in the bottom left-hand corner of both the plots. To explore this further, we plot in Fig. 9, V_{max} measured from the C IV absorption against $L_{2500\,\text{Å}}$. The Kendall τ-test gives a probability <0.01 per cent that V_{max} and $L_{2500\,\text{Å}}$ are not correlated both for the whole sample, sample excluding G06 sources, and the sample excluding both G06 and Giustini et al. (2008) sources. BAL quasars with high UV luminosities tend to have higher values of V_{max}. While there is a large range in V_{max}, for a given $L_{2500\,\text{Å}}$ at $\log(L_{2500\,\text{Å}}) < 31$, there is a lack of objects with $V_{max} < 10^4$ km s^{-1} at the high-luminosity end. Thus, there seems to be a lower envelope, the presence of which dominates the above correlation. This seems to be also the case when we plot BI against $L_{2500\,\text{Å}}$ (see Fig. 10). The marginal correlation found between the two parameters may mainly be dominated by the absence of low-BI sources at high optical luminosity. The above results are also consistent with that found by Ganguly et al. (2007).

A relationship between V_{max} and luminosity is expected if the broad troughs originate in a radiatively driven wind. From the analysis of C IV absorptions in low-z Seyfert galaxies and high-z high-luminosity QSOs, Laor & Brandt (2002) have shown that radiation-pressure force multiplier increases with luminosity (see also Ganguly et al. 2007). If true, this could explain the lower envelopes seen here. However, our analysis also shows that there is a large scatter in BI and V_{max} at any given luminosity. This probably means that even if radiation pressure is the main driver of the flow, other parameters are important such as the launching radius, the shape of the ionizing spectrum, the mass of the wind, the properties of the confining medium, etc.
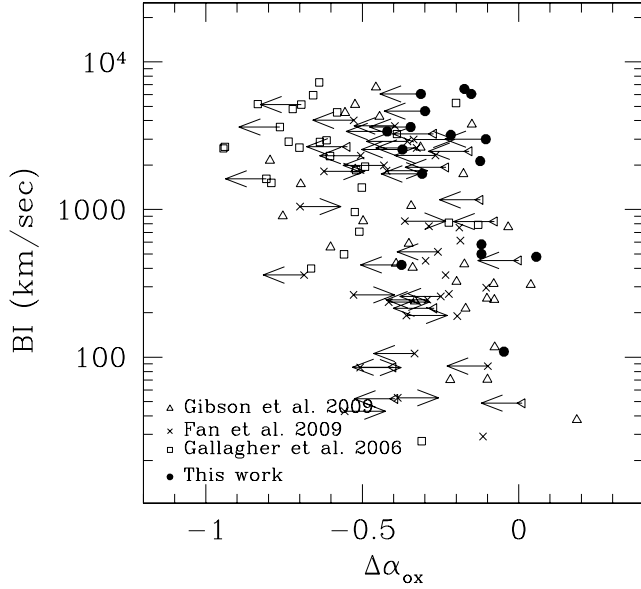
Figure 7. Correlation between BI and $\Delta\alpha_{ox}$ for various BAL quasar samples taken from the literature.

Table 2. Correlation analysis.

Variables	N-points	Kendall τ	
		τ	Probability (per cent)
V_{max} versus $\Delta\alpha_{ox}$	160	5.243	<0.01
V_{max} versus $L_{2500\,\text{Å}}$	160	4.421	<0.01
BI versus $\Delta\alpha_{ox}$	122	5.285	<0.01
BI versus $L_{2500\,\text{Å}}$	122	2.405	1.62
V_{max} versus $\Delta\alpha_{ox}$	131[a]	5.274	<0.01
V_{max} versus $L_{2500\,\text{Å}}$	131[a]	3.954	0.01
V_{max} versus $\Delta\alpha_{ox}$	93[b]	4.063	<0.01
V_{max} versus $L_{2500\,\text{Å}}$	93[b]	3.694	<0.01
BI versus $\Delta\alpha_{ox}$	93[a]	3.893	0.01
BI versus $L_{2500\,\text{Å}}$	93[a]	0.624	0.53

[a]Sample excluding data from G06.
[b]Sample excluding data from G06 and Giustini et al. (2008).

4.3 X-ray hardness ratio

The hardness ratio (HR) is often the only spectral information that is possible to extract when the X-ray source is weak. We queried the observations available in the *XMM–Newton* Science Archive version 6.0 (XSA) for all objects in our sample. For each observational ID, XSA provides the identified sources along with count rates and their associated errors in five energy bands. Thus, using XSA, we extracted the count rates for all our *XMM*-detected non-BAL and BAL quasars and estimated the HR between the soft (0.2–2 keV) and hard (2.0–10.0 keV) bands as

$$HR = \frac{C(2.0\text{–}12.0\,\text{keV}) - C(0.2\text{–}2.0\,\text{keV})}{C(2.0\text{–}12.0\,\text{keV}) + C(0.2\text{–}2.0\,\text{keV})}, \qquad (6)$$

where $C(2.0\text{–}12.0\,\text{keV})$ and $C(0.2\text{–}2.0\,\text{keV})$ are, respectively, the count rates in the 2.0–12.0 keV and 0.2–2.0 keV bands. The errors in HR were estimated by propagating the errors in each individual energy bands. In our sample, we have a total of 109 *XMM*-detected non-BAL quasars. Of these, the count rates were available for 106 sources. The average HR for these 106 sources is -0.61 ± 0.20. Similarly, of the eight *XMM*-detected BAL quasars, good count rates are available for seven *XMM* BAL quasars. The average HR
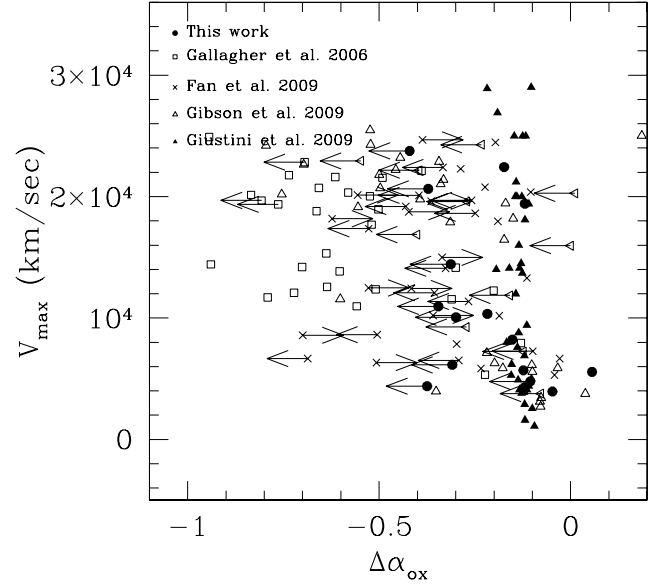
Figure 8. Maximum outflow velocity, V_{max} versus $\Delta\alpha_{ox}$ for BAL quasar samples collected from the literature.
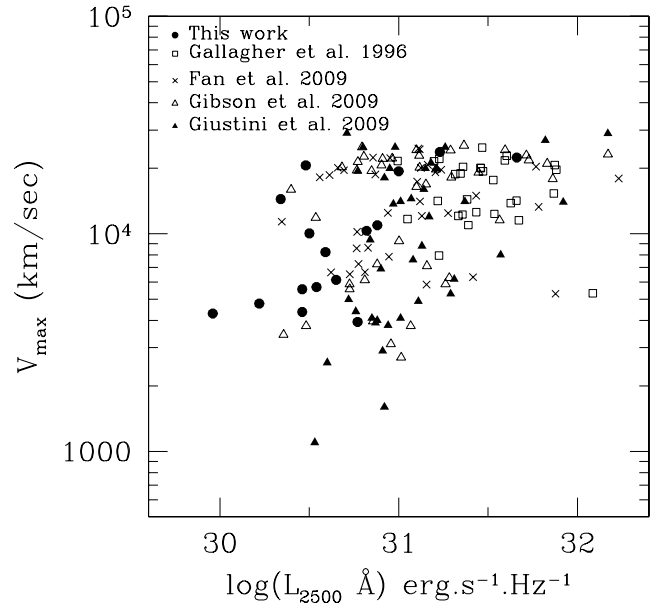
Figure 9. Maximum outflow velocity, V_{max}, versus the monochromatic luminosity at 2500 Å for various BAL quasar samples collected from the literature.

for these seven BAL quasars is -0.48 ± 0.20. The HR distributions for the *XMM*-detected BAL and non-BAL quasars are shown in Fig. 11. As the number of BAL quasars with X-ray detection is small, the trend of high HR in BAL quasars cannot be confirmed with any statistical significance.

4.4 X-ray spectral analysis

We also tried to perform a spectral analysis of archival *XMM* observations available for the eight BAL quasars. For this, we retrieved from XSA the original observational data file (ODF) for the eight sources. These data were then reduced using the *XMM* SAS (Science Analysis Software) version 8.0.1. The original event files
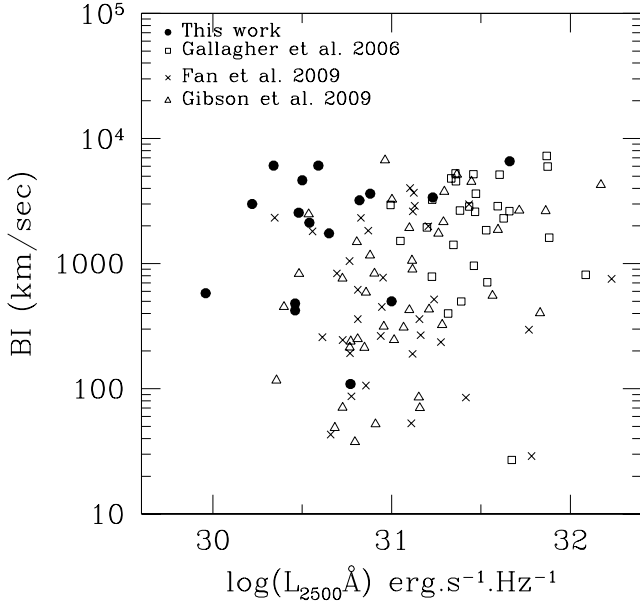
Figure 10. The BI is plotted versus the QSO monochromatic luminosity at 2500 Å for different samples of BAL quasars collected from the literature.
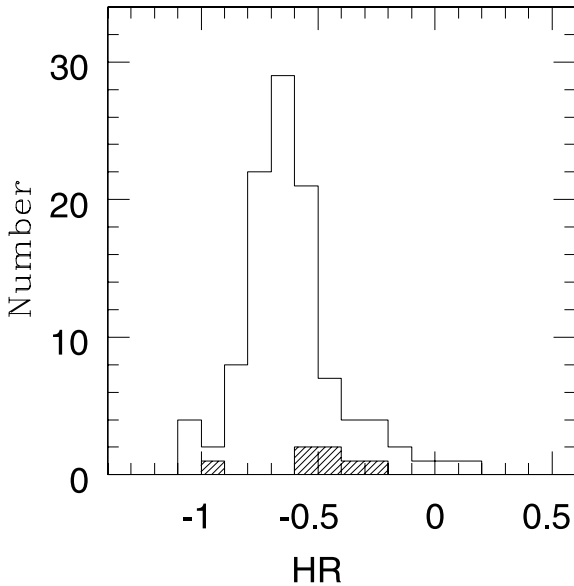

Figure 11. Distributions of the X-ray HR of the *XMM*-detected non-BALs (solid histogram) and BAL quasars (shaded histogram).

were filtered to retain only single-pixel and double-pixel events (PATTERN $\leq$ 4) as well as to retain only good quality events (FLAG = 0). From this filtered event file, time stamps having high background events were also removed. From the final cleaned event file, individual source spectra were generated for each *XMM*-detected BAL quasar with an extraction radius of 15–20 arcsec for the source and the background region. The background region was extracted from noise-free regions as close to the source as possible. Also, ancillary response file (ARF) and redistribution matrix file (RMF) at the position of the source were generated with the argen and rmfgen tasks. Total counts for each of these eight sources were extracted in the 0.2–8.0 keV region. Of these eight sources, only two sources have counts greater than 100, suitable for a reasonable spectral analysis. Therefore, for these two sources, spectra

were grouped in 15 count bin^{-1} and taken into xspec (Arnaud 1996) for spectral analysis. We performed the fit by minimizing χ^2. We model the spectra as a single power-law continuum emission with absorption. The observed and fitted spectra are shown in Fig. 12. For both sources, N_H values are found to be less than 10^{22} cm^{-2} and similar to the Galactic values. A similar conclusion was found by Giustini et al. (2008) when they fitted the spectra of their BAL sample assuming neutral absorbers. Recently, Streblyanska et al. (2010) found that about 36 per cent of their sample of BALs have low N_H when the spectra are fitted with a model including a neutral absorber. However, when the spectra are modelled with an ionized absorber, Streblyanska et al. (2010) found high values of N_H^i for more than 90 per cent of their sources. Due to the low count rates of the objects we study here, we are unable to apply such detailed models. Therefore, the N_H values reported here for the two X-ray-brightest objects in our sample should be treated as lower limits. For our two sources, we found photon index Γ values, 1.62 ± 0.44 and 2.80 ± 0.89, which are similar to those of typical radio-quiet quasars (Piconcelli et al. 2005) and within error of the mean photon index, $\Gamma = 1.87 \pm 0.21$, found from spectral analysis of 22 BAL quasars by Giustini et al. (2008). The results of our X-ray analysis on the eight BAL quasars are summarized in Table 3.

5 CONCLUSION

We have presented a new sample of 16 BAL quasars selected from a homogeneous sample of 159 $z_{em} > 1.5$, $g' < 22$ mag quasars found in a region of CFHTLS overlapping with the XMM-LSS and SWIRE surveys.

(i) We find a BAL quasar fraction of ~10 per cent in the whole sample and of ~8 per cent among optically selected quasars (120 quasars). This is similar to what is found from other optically selected quasar samples (Weymann et al. 1991; Hewett & Foltz 2003; Trump et al. 2006; Knigge et al. 2008; Gibson et al. 2009). Also, 7 per cent of the *XMM*-selected quasars are found to be BAL quasars. If we consider the 12 quasars which were selected from SWIRE colours only (and rejected by the optical colour selection), four are found to be BAL quasars which give a BAL fraction of ~33 per cent. This agrees with the large 23 per cent BAL quasar fraction found in 2MASS-selected quasars by Dai et al. (2008). We note here that recently Allen et al. (2010), after correcting for selection biases, report an intrinsic C IV BAL quasar fraction of ~41 $\pm$ 5 per cent, though their observed fraction is 8.0 $\pm$ 0.1 per cent.

(ii) The values of $\Delta\alpha_{ox}$, the deviation of the spectral index, α_{ox}, from the mean in the overall sample at the same UV luminosity, are distributed symmetrically around zero, whereas the $\Delta\alpha_{ox}$ values of *XMM*-detected BAL quasars are shifted towards lower values with an average of -0.169 ± 0.161. This shows that the X-ray-detected BAL quasars are weaker than the X-ray-detected non-BAL quasars by a factor of about 3. This X-ray weakness of BAL quasars compared to non-BAL quasars is similar to what was found in earlier studies (G06; Fan et al. 2009; Gibson et al. 2009); however, it contrasts with the results of Giustini et al. (2008). The discrepancy we find is however much less than what was reported by G06 who found that optically bright BAL quasars are X-ray sources weaker by a factor of 30 compared to non-BAL quasars. This might be due to the fact that G06 had used *Chandra* observations, reaching significantly fainter flux levels than the *XMM–Newton* observations used here for our sample of BALs.

(iii) We investigated various correlations between the properties of the C IV absorptions and α_{ox} using an extended sample gathered
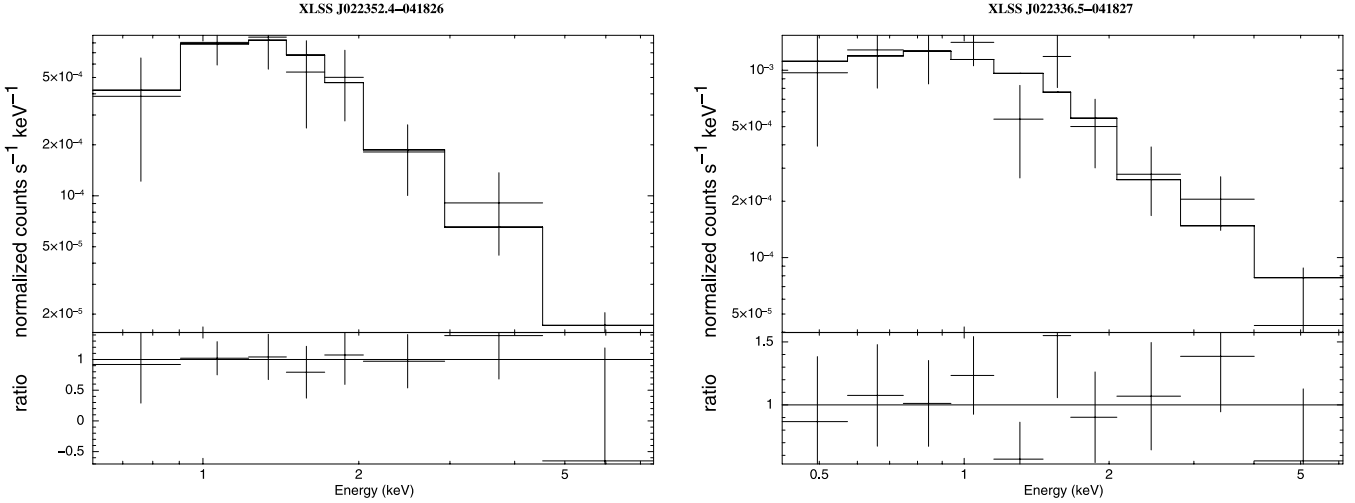
Figure 12. The observed and the fitted spectra of the two *XMM*-detected BAL quasars with counts larger than 100.

Table 3. X-ray spectral properties of the *XMM*-detected BAL quasars. Columns are as follows: (1) the *XMM* name; (2) the *XMM* observation ID; (3) the HR measured between 0.2–2.0 keV and 2.0–12.0 keV; (4) the Galactic neutral column density derived from Dickey & Lockman (1990); (5) the neutral column density from the spectral fit and (6) the fitted photon spectral index.

Name	Observation ID	HR	$N_{\mathrm{H,Gal}}$ (10^{20}) (cm^{-2})	N_{H} (10^{20}) (cm^{-2})	Γ
XLSS J022302.3−044437	0109520501	0.63 ± 1.09	2.68		
XLSS J022352.4−041826	0210490101	-0.52 ± 0.17	2.54	6.04 ± 0.33	2.80 ± 0.89
XLSS J022624.7−040458	0112680201	-0.28 ± 0.33	2.65		
XLSS J022647.7−041426	0112680101	-0.33 ± 0.27	2.66		
XLSS J022645.4−043615	0112681301	-0.41 ± 0.23	2.46		
XLSS J022257.2−042953	0109520601	-0.50 ± 0.55	2.63		
XLSS J022132.9−043750	0112680801	-0.90 ± 0.59	2.58		
XLSS J022336.5−041827	0210490101	-0.45 ± 0.10	2.55	0.97 ± 0.11	1.62 ± 0.44

after combining our data with those of G06, Giustini et al. (2008), Gibson et al. (2009) and Fan et al. (2009). For this large HiBAL quasar sample, $\Delta\alpha_{\mathrm{ox}}$ was calculated, and we find it to be correlated with the BI and the maximum velocity of the outflow, V_{max}. Similarly, V_{max} and BI are correlated with the 2500 Å monochromatic luminosity, $L_{2500\,\text{Å}}$. This suggests that quasars with high-velocity outflows are X-ray weak. While there is a large range in V_{max}, for a given $L_{2500\,\text{Å}}$ at $\log(L_{2500\,\text{Å}}) < 31$, there is a lack of objects with $V_{\mathrm{max}} < 10^4 \,\mathrm{km\,s}^{-1}$ at the high-luminosity end. Thus there seems to be a lower envelope, the presence of which dominates the above correlation. This probably means that even if radiation pressure is the main driver of the flow, other parameters, such as the launching radius, the shape of the ionizing spectrum, the mass of the wind, the properties of the confining medium, etc., are important.

(iv) We find the mean X-ray HR of the *XMM*-detected non-BAL and BAL quasars to be -0.61 ± 0.20 and -0.49 ± 0.20, respectively. While this is consistent with the assumption that X-ray weakness is due to soft X-ray absorption, the number of X-ray-detected BAL quasars is too small to make any statistically significant claim.

(v) The fit of the X-ray spectra from two BAL quasars shows that they have neutral hydrogen column densities smaller than $10^{22}\,\mathrm{cm}^{-2}$ and close to the Galactic values. This is based on a fully covering neutral absorber model. However, if the absorber is ionized and/or partially covering the X-ray source, the column density derived for these two BAL quasars should be considered lower limits. For these

two BAL quasars, the photon spectral index is found to be similar to that of radio-quiet quasars. This agrees with the photon index values found recently from X-ray spectral analysis of a larger sample of BAL quasars (Giustini et al. 2008; Streblyanska et al. 2010).

REFERENCES

Allen J. T., Hewett P. C., Maddox N., Richards G. T., Belokurov V., 2011, MNRAS, 410, 860
Anderson S. F. et al., 2007, AJ, 133, 313

Arav N., Li Z.-Y., Begelman M. C., 1994, ApJ, 432, 62

Arnaud K. A., 1996, in Jacoby G. H., Barnes J., eds, ASP Conf. Ser. Vol. 101, Astronomical Data Analysis Software and Systems V. Astron. Soc. Pac., San Francisco, p. 17

Becker R. H., White R. L., Gregg M. D., Brotherton M. S., Laurent-Muehleisen S. A., Arav N., 2000, ApJ, 538, 72

Bolzonella M., Miralles J. M., Pellò R., 2000, A&A, 363, 476

Brotherton M. S., Laurent-Muehleisen S. A., Becker R. H., Gregg M. D., Telis G., White R. L., Shang Z., 2005, AJ, 130, 2006

Dai X., Shankar F., Sivakoff G. R., 2008, ApJ, 672, 108

Dickey J. M., Lockman F. J., 1990, ARA&A, 28, 385

DiPompeo M. A., Brotherton M. S., Becker R. H., Tran H. D., Gregg M. D., White R. L., Laurent-Auehleisen S. A., 2010, ApJS, 189, 83

Fan L. L., Wang H. Y., Wang T., Wang J., Dong X., Zhang K., Cheng F., 2009, ApJ, 690, 1006

Gallagher S. C., Brandt W. N., Chartas G., Garmire G. P., 2002, ApJ, 567, 37

Gallagher S. C., Brandt W. N., Chartas G., Priddey R., Garmire G. P., Sambruna R. M., 2006, ApJ, 644, 709 (G06)

Gallagher S. C., Hines D. C., Blaylock M., Priddey R. S., Brandt W. N., Egami E. E., 2007, ApJ, 665, 157

Ganguly R., Brotherton M. S., Cales S., Scoggins B., Shang Z., Vestergaard M., 2007, ApJ, 665, 990

Ghosh K. K., Punsly B., 2008, ApJ, 674, L69

Gibson R. et al., 2009, ApJ, 692, 758

Giustini M., Cappi M., Vignali C., 2008, A&A, 491, 425

Goodrich R. W., Miller J. S., 1995, ApJ, 448, L73

Green P. J., Mathur S., 1996, ApJ, 462, 637

Green P. J. et al., 1995, ApJ, 450, 51

Green P. J., Aldcroft T. L., Mathur S., Wilkes B. J., Elvis M., 2001, ApJ, 558, 109

Green P. J. et al., 2009, ApJ, 690, 644

Gupta N., Srianand R., Petitjean P., Ledoux C., 2003, A&A, 406, 65

Hazard C., Morton D. C., Terlevich R., McMohan R., 1984, ApJ, 282, 33

Hewett P. C., Foltz C. B., 2003, AJ, 125, 1784

Hines D. C., Wills B. J., 1995, ApJ, 448, L69

Hutsemekers D., Lamy H., Remy M., 1998, A&A, 340, 371

Just D. W., Brandt W. N., Shemmer O., Steffen A. T., Schneider D. P., Chartas G., Garmire G. P., 2007, ApJ, 665, 1004

Knigge C., Scaringi S., Goad M. R., Cottis C. E., 2008, MNRAS, 386, 1426

Laor A., Brandt W. N., 2002, ApJ, 569, 641

Laor A., Fiore F., Elvis M., Wilkes B. J., McDowell J. C., 1997, ApJ, 477, 93

Lavalley M., Isobe T., Feigelson E., 1992, in Worall D. M., Biemesderfer C., Barnes J., eds, ASP Conf. Ser. Vol. 25, Astronomical Data Analysis Software and Systems I. Astron. Soc. Pac., San Francisco, p. 245

Lonsdale C. J. et al., 2003, PASP, 115, 897

Mathur S. et al., 2000, ApJ, 533, L79

Miller B. P., Brandt W. N., Gibson R. R., Garmire G. P., Shemmer O., 2009, ApJ, 702, 911

Murray N., Chiang J., 1995, ApJ, 454, L105

Oke J. B., Gunn J. E., 1983, ApJ, 266, 713

Piconcelli E., Jimenez-Bailón E., Guainazzi M., Schartel N., Rodríguez-Pascual P. M., Santos-Lleó M., 2005, A&A, 432, 15

Pierre M. et al., 2004, J. Cosmol. Astropart. Phys., 09, 011

Pierre M. et al., 2007, MNRAS, 382, 279

Priddey R. S., Gallagher S. C., Issak K. G., Sharp R. G., McMohan R. G., Butner H. M., 2007, MNRAS 374, 867

Proga D., Stone J. M., Kallman T. R., 2000, 543, 686

Reichard T. A. et al., 2003, AJ, 126, 2594

Richards G. T. et al., 2002, AJ, 123, 2945

Sabra B. M., Hamann F., 2001, ApJ, 563, 555

Schmidt G. D., Hines D. C., 1999, ApJ, 512, 125

Shankar F., Dai X., Sivakoff G. R., 2008, ApJ, 687, 859

Sharp R. et al., 2006, in McLean I. S., Iye M., eds, Proc. SPIE Vol. 6269, Ground-based and Airborne Instrumentation for Astronomy. SPIE, Bellingham, p. 62690G

Sprayberry D., Foltz C. B., 1992, ApJ, 390, 39

Srianand R., Petitjean P., 2000, A&A, 357, 414

Srianand R., Petitjean P., Ledoux C., Hazard C., 2002, MNRAS, 336, 753

Stalin C. S., Petitjean P., Srianand R., Fox A. J., Coppolani F., Schwope A., 2010, MNRAS, 401, 294

Steffen A. T., Strateva I., Brandt W. N., Alexander D. M., Koekemoer A. M., Lehmer B. D., Schneider D. P., Vignali C., 2006, AJ, 131, 2826

Stern D., Djorgovski S. G., Perley R. A., de Carvalho R. R., Wall J. V., 2000, AJ, 119, 1526

Stern D. et al., 2005, ApJ, 631, 163

Streblyanska A., Barcons X., Carrera F. J., Gil-Merino R., 2010, A&A, 515, 2

Tolea A., Krolik J. H., Tsvetanov Z., 2002, ApJ, 578, 31

Trump J. R. et al., 2006, ApJS, 165, 1

Urrutia T., Becker R. H., White R. L., Glikman E., Lacy M., Hodge J., Gregg M. D., 2009, ApJ, 698, 1095

Wampler E. J., Chugai N. N., Petitjean P., 1995, ApJ, 443, 586

Wang J., Jiang P., Zhou H., Wang T., Dong X., Wang H., 2008, ApJ, 676, L97

Weymann R. J., Morris S. L., Foltz C. B., Hewett P. C., 1991, ApJ, 373, 23

Willott C., Rawlings S., Grimes J. A., 2003, ApJ, 598, 909

This paper has been typeset from a TEX/LATEX file prepared by the author.